Zhang *et al.*
Chinese Journal of Mechanical Engineering (2021) 34:115
https://doi.org/10.1186/s10033-021-00640-w

Chinese Journal of Mechanical Engineering

ORIGINAL ARTICLE

Open Access

Effect of Thermal Cyclic Loading on Stress-Strain Response and Fatigue Life of 3D Chip Stacking Structure

Liang Zhang[1,2*], Weimin Long[1] and Sujuan Zhong[1]

Abstract

The thermo-mechanical reliability of IMCs (Ni_3Sn_4, Cu_3Sn, Cu_6Sn_5) solder joints and Sn-3.9Ag-0.6Cu solder joints was investigated systematically in 3D chip stacking structure subjected to an accelerated thermal cyclic loading based on finite element simulation and Taguchi method. Effects of different control factors, including high temperature, low temperature, dwell time of thermal cyclic loading, and different IMCs on the stress-strain response and fatigue life of solder joints were calculated respectively. The results indicate that maximum stress-strain can be found in the second solder joint on the diagonal of IMC solder joints array; for Sn-3.9Ag-0.6Cu solder joints array, the corner solder joints show the obvious maximum stress-strain, these areas are the crack propagated locations. The stress-strain and fatigue life of solder joints is more sensitive to dwell temperature, especially to high temperature; increasing the high temperature, dwell time, or decreasing the low temperature, can reduce the stress-strain and enlarge the fatigue life of solder joints. Finally, the optimal design in the 3D-IC structure has the combination of the Cu_6Sn_5/Cu_3Sn, 373 K high temperature, 233 K low temperature, and 10 min dwell time. The fatigue lives of Sn-3.9Ag-0.6Cu under 218–398 K loading in the 3D assembly based on the creep strain are 347.4 cycles, which is in good agreement with experimental results (380 cycles).

Keywords: 3D-IC, Taguchi method, Control factors, Fatigue life

1 Introduction

With the development of chip technology, the use of Moore's law in microelectronic industry may approach the limit, three-dimensional integrated circuits (3D-IC) technology can overcome the limitations of Moore's law with the advantage of high density integration, high performance and low power consumption [1–3]. Therefore, the chip stacking in 3D-IC has attracted considerable attention in electronic industry, and different bonding technologies have been developed to ensure the chip (or wafer) vertical stacking. Among the bonding technologies, TLP bonding with solder has been proposed as an effective method to implement low temperature bonding and high temperature service.

Talebanpour et al. [4] used Sn-3.0Ag-0.5Cu as interconnection materials in 3D structure with 260℃ reflow temperature and aging to obtain total IMC (Cu_6Sn_5/Cu_3Sn). Chu et al. [5] investigated Cu/Sn/Cu and Ni/Sn/Ni solder joints for low temperature stable transient liquid phase (TLP) bonding, Cu_6Sn_5, Cu_3Sn, Ni_3Sn_4, Ni_3Sn_2 can be detected respectively. Chen et al. [6] investigated the Cu/Sn3.5Ag/Cu and Cu/Sn3.5Ag/Cu15Zn based on TLP bonding; Cu_6Sn_5 and $Cu_6(Sn, Zn)_5$ were found in the solder joints, and it is found that the Cu_6Sn_5 can weaken the bond reliability resulting from its homogeneous grain structure and brittleness. The Zn can effectively modify the homogeneous grain structure into interfolded structure to enhances the bond reliability. Moreover, Sn-Bi solder can be selected to conduct the complete Cu_3Sn

*Correspondence: zhangliang@jsnu.edu.cn
[1] Zhengzhou Research Institute of Mechanical Engineering Co., LTD, Zhengzhou 450001, China
Full list of author information is available at the end of the article

Springer Open

© The Author(s) 2021. **Open Access** This article is licensed under a Creative Commons Attribution 4.0 International License, which permits use, sharing, adaptation, distribution and reproduction in any medium or format, as long as you give appropriate credit to the original author(s) and the source, provide a link to the Creative Commons licence, and indicate if changes were made. The images or other third party material in this article are included in the article's Creative Commons licence, unless indicated otherwise in a credit line to the material. If material is not included in the article's Creative Commons licence and your intended use is not permitted by statutory regulation or exceeds the permitted use, you will need to obtain permission directly from the copyright holder. To view a copy of this licence, visit http://creativecommons.org/licenses/by/4.0/.

solder joints for 3D IC [7]; the Ni_3Sn_4 solder joints can also achieve 3D bonding [8]. In 3D IC structure, the reliability of complete IMC solder joints under thermal cycling loading, has been considered as an important research aspect; the finite element code can be used to calculate the stress-strain response and fatigue life of IMC solder joints. Tian et al. [9] researched the stress analysis and structure optimized of IMC joints in 3D package with finite element simulation; it is found that the resin thickness plays the most important role and the resin hardness plays the least important role in affecting the stress in the IMC joint. Lee et al. [10] investigated the stress-strain of Sn-Ag solder joints in 3D IC, and the effect of chip thickness and TSV pitch on the inelastic strain has been studied systematically using finite element code. The finite element simulation is an effective way to analyze the stress-strain response and fatigue life of solder joints in electronic field [11], however, no publication reported the effect of different IMCs on the reliability of solder joints in 3D IC.

In this paper, the IMCs and Sn-3.9Ag-0.6Cu solder joints were considered in 3D-IC; the effect of high temperature, low temperature, dwell time of thermal cyclic loading, and different IMCs on the solder joints reliability during thermal cyclic loading was studied using finite element method (FEM) and Taguchi method. The results can provide an effective way to evaluate the reliability of IMC and Sn-3.9Ag-0.6Cu solder joints in 3D-IC.

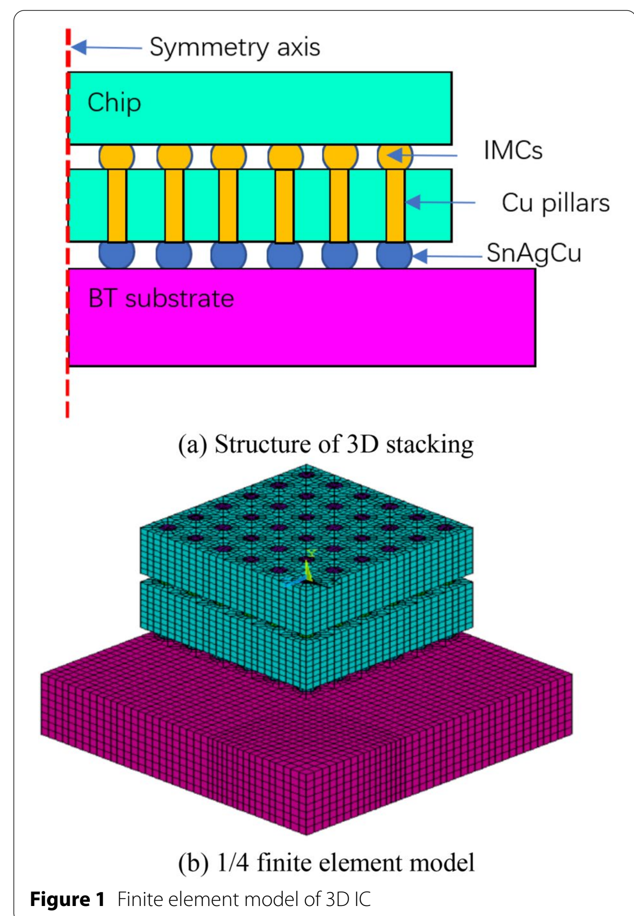

Figure 1 Finite element model of 3D IC

2 FEM Analysis

In 3D-ICs, the most significant elements of the enabling technology for handling and double-sided processing of extremely thin chips are the temporary bonding and debonding processes at a lower temperature and a higher throughput [12]. A common 3D device is shown in Figure 1; the two chips are bonded to form IMCs solder joints via TLP bonding, then the assembly is soldered on BT substrate with Sn-3.9Ag-0.6Cu alloy using reflow soldering bonding. Meanwhile, during the second bonding, the first-level IMCs solder joints will not be molten and keep stable state. Since the process of thermal cycling test is time consuming with high cost, the FE simulation is adopted to analyze the mechanics and reliability of materials and structures in electronic package especially during the design stage [13]. FEM has been proposed by many researchers to calculate the stress-strain and to predict the reliability of solder joints. Due to the symmetry in the geometry, the quarter symmetric finite element model of the 3D-IC was utilized, which can reduce the computational time. The quarter models have been utilized in BGA, CSP, WLCSP and QFP devices successfully in finite element simulation to calculate the fatigue life of solder joints under thermal cycle loading [14–16].

As shown in Figure 1(b), the 3D IC model consists of chips, IMCs/Sn-3.9Ag-0.6Cu solder joints, TSV Cu pillars, BT substrate and Cu/Ni pads. SOLID186 with 20-node hexahedral element was selected to model the complex geometry in order to calculate the stress-strain response; sweep mesh method was utilized in modeling, and the element number is 896670. Since we only focus on the solder joints, a finer mesh is adopted to model the 3D assembly. Figure 2 shows the IMCs solder joints and Sn-3.9Ag-0.6Cu lead-free solder joints array. Meanwhile, the displacement boundary conditions are considered; zero displacement constraints of vertical direction of the cross-area are applied to the cross-sections of the quarter model, namely, all nodes on the symmetric surface ($X=0$, $Z=0$) are fixed in the corresponding directions (X, Z), and the node at the origin ($X=Y=Z=0$) is constrained in all three directions.

Table 1 shows the material parameters of the chip, IMCs solder joint, Ni/Cu pads and BT substrate in 3D assembly; these material parameters are assumed to be isotropic, linearly elastic and independent of temperature except for those of Sn-3.9Ag-0.6Cu solders [17]. It is well

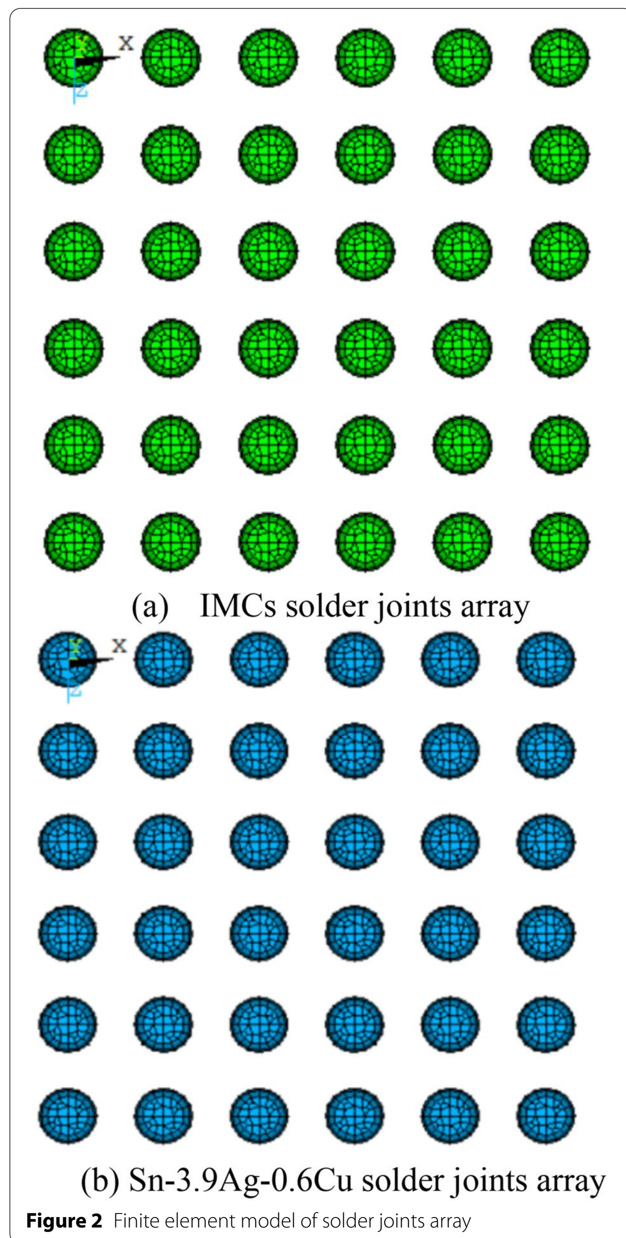

Figure 2 Finite element model of solder joints array

Table 1 Parameters of materials

Materials	*E* (MPa)	*μ*	CTE ($\times 10^{-6}$K^{-1})
Sn-3.9Ag-0.6Cu	43700-22.3T	0.40	20.9
Chip	163000	0.28	2.5
BT	26000	0.39	15.0
Cu	117000	0.23	16.6
Ni	207000	0.31	13.1
Cu_3Sn	143000	0.30	18.2
Cu_6Sn_5	124000	0.30	19.0
Ni_3Sn_4	134000	0.33	13.7

demonstrated that creep plays a very important role in deformation behavior of materials, when the homologous temperature is close to 0.5 or above with slow loading, creep deformations will occur [18]. The Sn-3.9Ag-0.6Cu lead-free alloy is subjected to high homologous temperatures (0.61) at room temperature. Therefore, the creep response may be considered as the main deformation of solder joints in service. In the FE simulation, Garofalo-Arrhenius model is employed extensively to describe the steady-state creep of lead-free solder alloys [19]; Eq. (1) shows the creep model to calculate the creep behavior of Sn-3.9Ag-0.6Cu solders.

$$\frac{\mathrm{d}\gamma}{\mathrm{d}t} = C\left(\frac{G}{T}\right)\left[\sinh\left(\omega\frac{\tau}{G}\right)\right]^n \exp\left(-\frac{Q}{RT}\right), \quad (1)$$

where $\mathrm{d}\gamma/\mathrm{d}t$ is the creep shear strain rate; G is the shear modulus; T is the absolute temperature; τ is the stress level; n is the stress exponent; R is the gas constant; Q is the activation energy; C and ω are the materials constant, respectively.

If the solder materials obey the von Mises criterion, the creep equation can be rearranged and expressed as Eq. (2) [20].

$$\dot{\varepsilon} = C_1[\sinh(C_2\sigma)]^{C_3} \exp\left(-\frac{C_4}{T}\right), \quad (2)$$

where $\dot{\varepsilon}$ is the equivalent creep strain rate; σ is the equivalent stress; T is the absolute temperature; C_1, C_2, C_3 and C_4 are the materials constants, which are given in Table 2 for Sn-Ag-Cu solder.

In evaluation of electronic device, accelerated thermal cycling tests are often utilized to speed up the thermal fatigue failure process, to assess the reliability of lead-free solder joints under cyclic temperature variation. According to the thermal cycling testing [21], temperature loading from 218 to 398 K is proposed to evaluate the reliability of IMCs and Sn-3.9Ag-0.6Cu lead-free solder joints in 3D-IC, and duration of thermal cycle is 60 min, including 15 min dwell at 218 K and 398 K, which is shown in Figure 3. In order to analyze the parameters on the reliability of solder joints, the high temperature, the low temperature, the dwell time of thermal cyclic loading are considered in FE simulation; during the analysis, the variation of high temperature, low temperature and dwell time are considered, and the duration of thermal cycle still is 60 min. In addition, it is assumed that at all nodes in the 3D assembly are

Table 2 Parameters of creep

Materials	C_1 (s^{-1})	C_2 (MPa^{-1})	C_3	C_4 (K)
Sn-3.9Ag-0.6Cu	441000	5×10^{-9}	4.2	5412

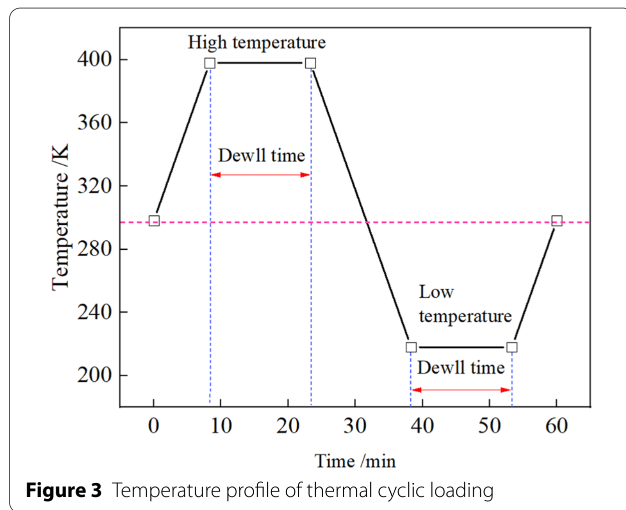

Figure 3 Temperature profile of thermal cyclic loading

subjected to no stress at the initial temperature, and loaded a uniform temperature distribution in the finite element simulation. The assumption has been utilized in Refs. [22, 23], which can simplify the calculation time in finite element simulation.

3 Results and Discussions

Figure 4 plots the von Mises stress and von Mises total mechanical strain of IMCs solder joints in 3D assembly, and the maximum strain-strain is obtained in the second IMC solder joint of the chip oriented diagonally; demonstrating the diagonal position is more critical than the rectangular one. However, the stress-strain response of IMC solder joints is different from that of Sn-3.9Ag-0.6Cu solder joints. Figure 5 shows the von Mises stress and von Mises total mechanical strain of Sn-3.9Ag-0.6Cu solder joints in the array, indicating that the von Mises stress and von Mises total mechanical strain change obviously with the increase of distance to neutral point. In addition, the maximum stress and strain occur on the outer solder joint, and concentrate on the top surface of corner solder joint near the chip, the area may be the failure location of 3D assembly. In WLCSP device, Wu et al. [24] also found that the dangerous zone is the corner of the solder joint near the chip pad side, in addition, the crack extends in the location from experimental result, which demonstrates that the stress-strain response calculated can predict the failure location of solder joints.

Figure 6 shows the deformed shapes (500X) of the 3D assembly after three thermal cycles. The maximum displacement can be found in the Sn-3.9Ag-0.6Cu solder joint array, and it can be found with the increasing of the distance with the center solder joints. The displacement increases obviously; the displacement mainly concentrates at corner solder joints in the 3D assembly, due to the mismatch of thermal expansion coefficient between chip and substrate. The solder joints are subjected to great deformation, meanwhile, similar findings can be found in WLCSP device with Sn-2Ag-36Pb and Sn-3.5Ag solder joints [25].

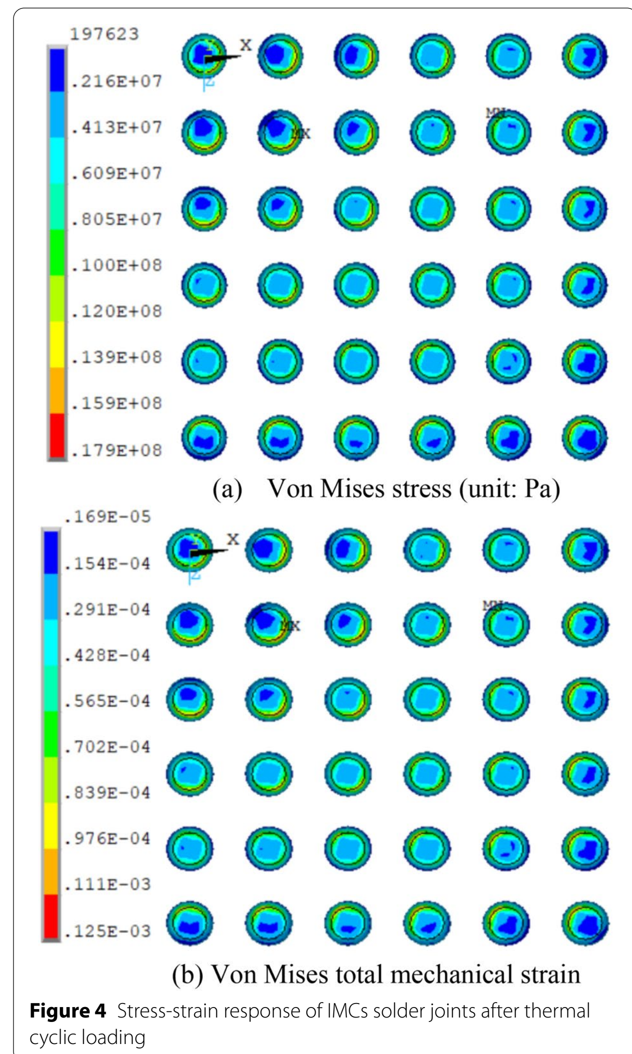

Figure 4 Stress-strain response of IMCs solder joints after thermal cyclic loading

The Taguchi method is widely used to analyze the factor level combination and to assess effect factors, so the method is selected in our research to determine the effect of different control factors on the reliability of solder joints in the 3D assembly. In 1980, Taguchi's introduction of robust design to several major American industries, including AT & T, Ford and Xerox, resulted in significant quality improvements in product and manufacturing process design [26]. For Taguchi method, the orthogonal array (OA) and signal-to-noise (S/N) ratio are the main instruments for economically conducting and analyzing an experiment [27]. The idea of orthogonal arrays is to get the statistic information and robust process

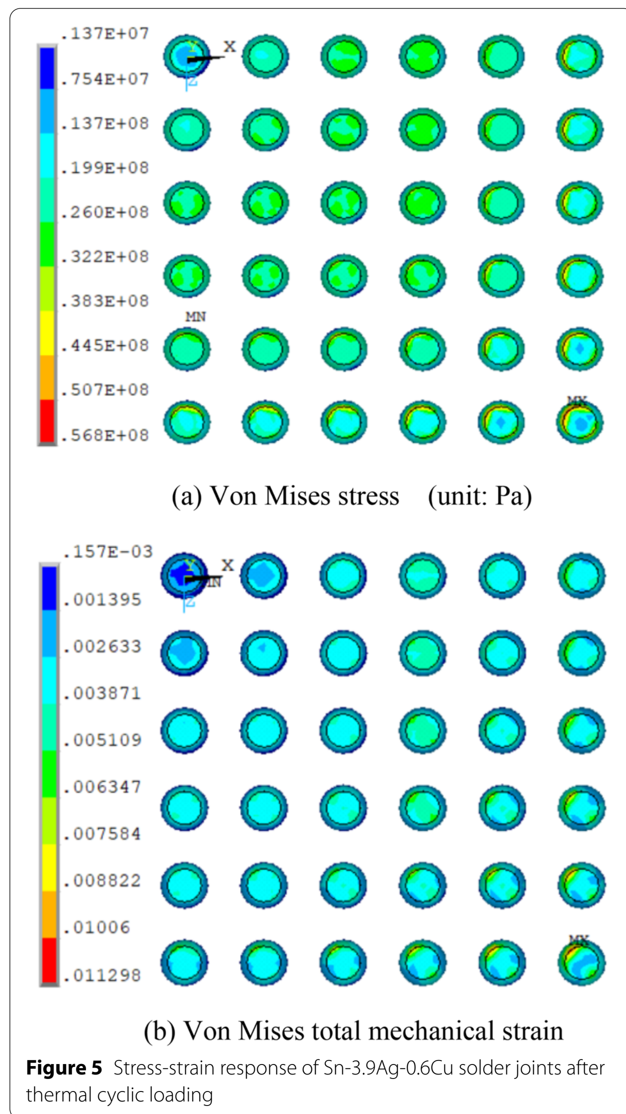

Figure 5 Stress-strain response of Sn-3.9Ag-0.6Cu solder joints after thermal cyclic loading

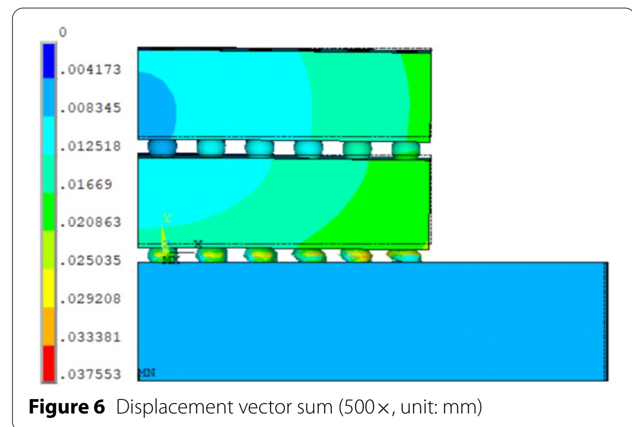

Figure 6 Displacement vector sum (500×, unit: mm)

conditions during shorter time by using fewer analyses. With the consideration of control factors and their levels, the L_9 (3^4) orthogonal array is to be used in the optimized experiment to minimize the creep strain $\Delta\varepsilon$. The robust design (or quality) characteristics can be classified into three different types: (1) Nominal-the best, (2) smaller-the-better, and (3) larger-the-better [28]. In 3D assembly, the design of the chip stacked structure, the stress-strain of the solder joints has to be minimized, the smaller-the-better criterion is suitable to describe the experimental results. The signal-to-noise (*S/N*) objective function for the quality characteristic of smaller-the-better type can be computed as shown in Eq. (3):

$$S/N = -10\lg\left(\frac{\sum_{i=1}^{r} y_i^2}{r}\right), \tag{3}$$

Table 3 Control factors and levels

Control factors		Level 1	Level 2	Level 3
A	IMC	Cu_6Sn_5	Cu_3Sn	N_3Sn_4
B	High Temperature (K)	423	398	373
C	Low Temperature (K)	233	218	213
D	Dwell time (min)	15	12.5	10

where r is the total number of measurements; y_i is the ith measurement data, and *S/N* is the signal-to-noise ratio in decibel.

In the finite element simulation, the $r=1$ and $y_1 = \Delta\varepsilon_1 = \Delta\varepsilon$, so $\frac{\sum_{i=1}^{r} y_i^2}{r} = \Delta\varepsilon^2$, therefore, the Eq. (3) can be transforms to

$$S/N = -10\lg\left(\Delta\varepsilon^2\right). \tag{4}$$

The four selected control factors and their levels applied in this study are tabulated in Table 3. These control factors contain high temperature, low temperature, dwell time of thermal cyclic loading, and different IMCs. And the control factors all show three levels. Cu_6Sn_5, Cu_3Sn and Ni_3Sn_4 IMCs are selected in this paper; these IMCs show higher melting temperatures than Sn-based alloys.

Taguchi method can effectively find out the optimal condition of production to ensure the consistency and get the best quality control with the lowest cost [29]. In order to obtain the optimal parameters of the 3D assembly, the main experiment is carried out to analyze the control factors and levels within Taguchi method. Table 4 shows the simulated creep strain ($\Delta\varepsilon$) and the S/N ratio for each experiment cells on the $L_9(3^4)$ orthogonal array. It is found that with the variation of high temperature, low temperature, dwell time of thermal cyclic loading,

Table 4 Main experiment

EXP.	Factor and level				Quality	
	A	B	C	D	$\Delta\varepsilon$	*S/N*
1	1	1	1	1	0.08422	21.49
2	1	2	2	2	0.07053	23.03
3	1	3	3	3	0.05579	25.07
4	2	1	2	3	0.08338	21.58
5	2	2	3	1	0.07061	23.02
6	2	3	1	2	0.05621	25.00
7	3	1	3	2	0.08382	21.53
8	3	2	1	3	0.06952	23.16
9	3	3	2	1	0.05707	24.87
Average						23.19

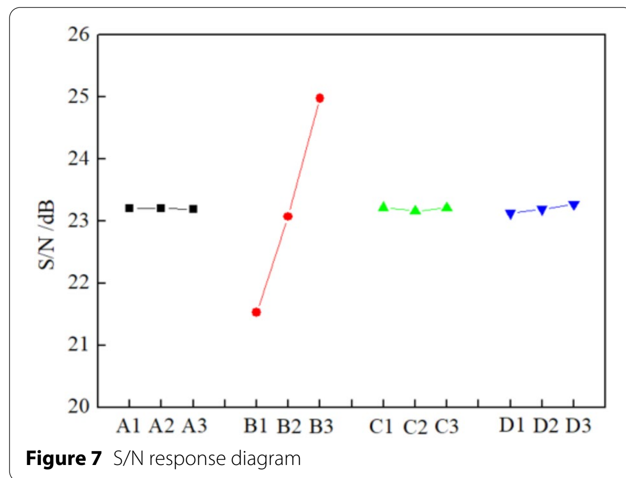

Figure 7 S/N response diagram

and different IMCs, the creep strain ($\Delta\varepsilon$) and *S/N* ratio change significantly. The smaller values of creep strain ($\Delta\varepsilon$) demonstrate that the more reliability of Sn-3.9Ag-0.6Cu solder joints in 3D assembly. And the evaluation of Sn-3.9Ag-0.6Cu solder joints is based on the quality factor $\Delta\varepsilon$.

Figure 7 shows the S/N ratio response diagram of the four control factors; magnitudes of the control factors response and ranks are summarized in Table 5. According to the S/N response diagram, the greater the S/N ratio is, the smaller the variation of equivalent creep strain will be. The effect of four factors is different, and the contribution degree of the four factors is Factor B (High Temperature) > Factor D(Dwell time) > C(Low Temperature) >Factor A(IMCs). The most important factor is the high temperature, which demonstrates that the reliability of the Sn-Ag-Cu solder joints in 3D assembly can be influenced mainly by high temperature of thermal cycles loading. Other three parameters have small impact on the reliability, especially for IMCs, and we

Table 5 S/N response and rank

	Factor and level			
	A	B	C	D
Level 1	23.20	21.53	23.22	23.13
Level 2	23.20	23.07	23.16	23.19
Level 3	23.19	24.98	23.21	23.27
Effect	0.01	3.45	0.06	0.14
Rank	4	1	3	2

should enhance the reliability of Sn-Ag-Cu solder joints based on the optimal design. The optimal parameters match is A1/2B3C1D3, namely, the optimal design in the 3D assembly has the combination of the Cu_6Sn_5/Cu_3Sn, high temperature at 373 K, low temperature at 233 K, dwell time at 10 min. Moreover, it is imperative to illustrate that when the levels are varied, the optimal set of the control factors and rank then change obviously. The effect deviation of factor (IMCs) on S/N repose is very small and negligible.

Figure 8 shows the two different temperature profiles of thermal cyclic loading to analyze the stress-strain response of solder joints. For the two different temperature profiles of thermal cycle loading, the durations of thermal cycle are 60 min, and only high temperature, low temperature, dwell time are different. Based on the finite element simulation combined with Taguchi method, only high temperature can affect the reliability of solder joints. When high temperature (*T*) changes obviously, the ramp rate ($\mathrm{r} = T/s$) will also vary. Therefore, in this paper, high temperature and ramp rate have same effect, only high temperature was selected as an analyzed parameter.

Figure 9 shows the history of von Mises stress and equivalent creep strain history at the corner Sn-3.9Ag-0.6Cu solder joints of the 3D assembly, respectively.

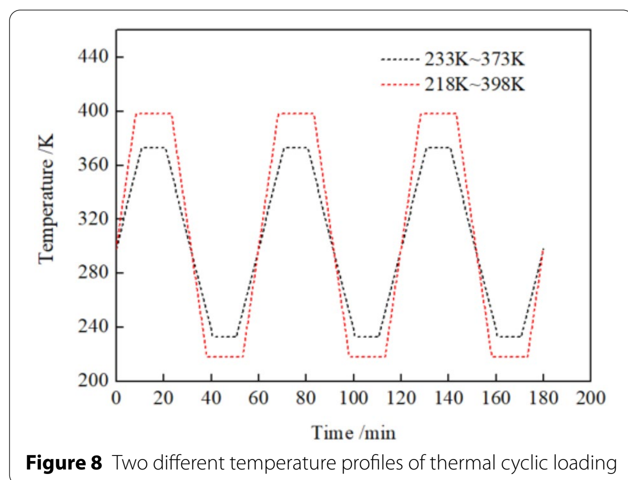

Figure 8 Two different temperature profiles of thermal cyclic loading

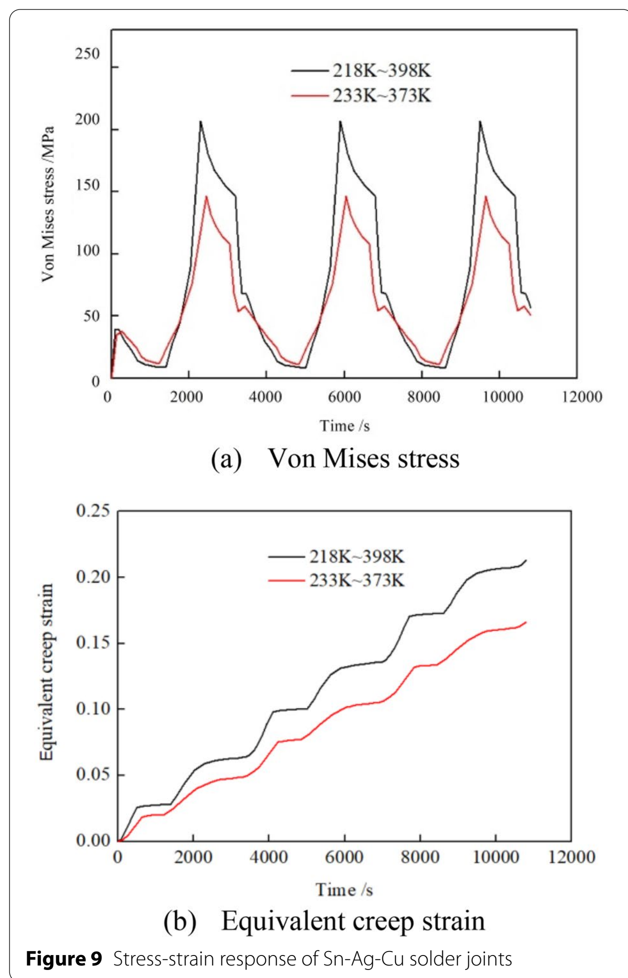

Figure 9 Stress-strain response of Sn-Ag-Cu solder joints

The von Mises stress and equivalent creep strain history of Sn-3.9Ag-0.6Cu solder joints under 218–398 K loading is higher than that of solder joints under 233–373 K loading. It demonstrates that the decrease of high temperature can decrease the von Mises stress and equivalent creep strain history under thermal cycling. Moreover, a low stress can be found in the von Mises stress curve during the high temperature stage of the thermal cyclic loading, whereas a high stress appears in the low temperature stage. Due to creep effect, stress relaxation happens both at the high and low temperature dwell stage. For the second and third thermal cycle, the Sn-3.9Ag-0.6Cu solder joints reach a stabilized cyclic pattern, in which the highest stress is experienced at the beginning of the low temperature dwell. But the lowest stress at the end of the high temperature dwell due to the viscous behavior of the solder joints. Meanwhile, both equivalent creep strain increases as the temperature cycle proceeds, and the thermally induced cyclic creep deformation tends to accumulate as the number of the thermal cycle increase. The creep strain of Sn-3.9Ag-0.6Cu solder joints under 218–398 K loading is higher than that of solder joints under 233–373 K loading, which can be attributed to the enhancement of creep strain with the increase of high temperature. Moreover, the high temperature increases significantly, as well as the ramp rate, and the equivalent creep strain will be boosted.

With the FM simulated and the fatigue life equation, the Sn-3.9Ag-0.6Cu solder joints in 3D assembly can be calculated effectively. A number of fatigue life prediction models have been proposed in electronic packaging field, and the prediction equations based on accumulated creep strain show obvious superiority. Syed et al. [30] suggests that creep is the primary damage mechanism for Sn-Ag-Cu solder during thermal cycling, and can be used to simulate the material's behavior. So the creep deformation can be considered in the life prediction model. Fatigue life prediction equation of Sn3.9Ag-0.6Cu solder joints based on accumulated creep strain is as Eq. (5) [31].

$$N_f = (0.0405\Delta\varepsilon)^{-1}, \tag{5}$$

where N_f is the number of cycles to failure, $\Delta\varepsilon$ is the accumulated creep strain per cycle.

The fatigue lives of Sn-3.9Ag-0.6Cu under 218–398 K and 233–373 K loading in the 3D assembly based on the creep strain are 347.4 cycles and 445.5 cycles, which demonstrates that the increase of high temperature of the thermal cycles loading can increase the equivalent creep strain and reduce the fatigue life of Sn-3.9Ag-0.6Cu solder joints in 3D assembly. Figure 10 shows the crack of solder joint in experiments (380 cycles, 218–398 K); the results have a good agreement with the simulated result to predict the failure location. Due to the mismatch of thermal expansion coefficient between

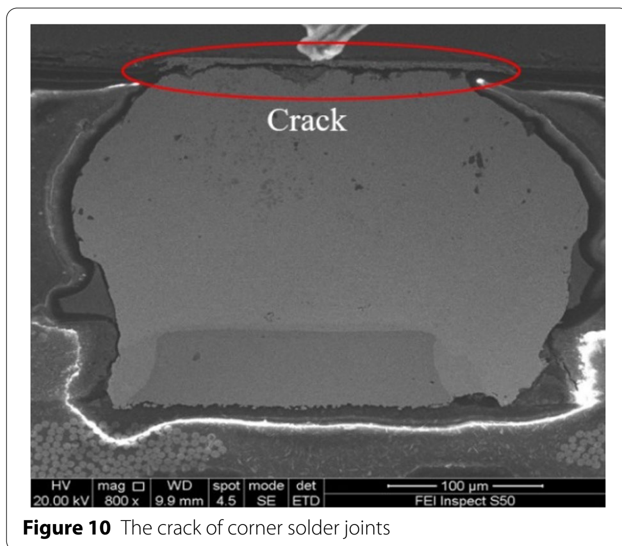

Figure 10 The crack of corner solder joints

chip and substrate, the solder joint is subjected to creep strain, when the accumulated creep strain reaches a critical value, the crack may initial and propagate. Moreover, due to thermal cycling loadings, the IMC growth can be found at the interface; overly thick brittle IMCs can also become apparent as a crack initiation zone for the entire solder joint. Therefore, the investigation of IMC growth and inhibition [32, 33] become the important topic in electronic packaging field.

4 Conclusions

(1) According to the results of stress-strain response of IMCs (Ni_3Sn_4, Cu_3Sn and Cu_6Sn_5) solder joints and Sn-3.9Ag0.6Cu solder joints in 3D assembly using finite element simulation, the von Mises stress and von Mises total mechanical strain change obviously with the increase of distance to neutral point, the maximum stress and strain occur on the outer solder joint, and concentrate on the top surface of corner solder joint near the chip.

(2) The results indicate that the high temperature is most important factor among all the four control factors (high temperature, low temperature, dwell time of thermal cyclic loading, and different IMCs).

(3) The stress-strain response and fatigue life of the Sn-3.9Ag-0.6Cu solder joints in 3D assembly can be influenced mainly by high temperature of thermal cycles loading, other three parameters have small impact on the reliability, especially for IMCs.

Acknowledgements
The authors would like to thank Dr. Wang Xiao, Jiangsu Normal University, Xuzhou, PRC for critical review of the paper.

Authors' Contributions
LZ was in charge of the whole trial and wrote the manuscript; WL and SZ assisted with sampling and laboratory analyses. All authors read and approved the final manuscript.

Authors' Information
Liang Zhang, born in 1984, is currently a professor at *Jiangsu Normal University, China*. He received his PhD degree from *Nanjing University of Aeronautics and Astronautics, China*, in 2011. His research interests include electronic packaging technology, lead-free solders and technology, brazing and related reliability.
Weimin Long, born in 1966, is currently a senior scientist at *Zhengzhou Research Institute of Mechanical Engineering Co., LTD, China*. He received his master degree on *Materials Processing Engineering in Tsinghua University, China*, in 2003.
Sujuan Zhong, born in 1974, is currently a senior scientist at *Zhengzhou Research Institute of Mechanical Engineering Co., LTD, China*. She received his master degree on *Powder Metallurgy in Central South University, China*, in 2000.

Funding
Supported by State Key Lab of Advanced Welding and Joining, Harbin Institute of Technology (Grant No. AWJ-19Z04), Major State Research Development Program of China (Grant No.2019YFF0217400), the Central Plains Science and Technology Innovation Leading Talents Program (Grant No.ZYQR20180030).

Competing Interests
The authors declare no competing financial interests.

Author Details
[1]Zhengzhou Research Institute of Mechanical Engineering Co., LTD, Zhengzhou 450001, China. [2]School of Mechatronic Engineering, Jiangsu Normal University, Xuzhou 221116, China.

Received: 21 July 2020 Revised: 30 August 2021 Accepted: 3 November 2021
Published online: 27 November 2021

References

[1] L Zhang, Z Liu, S Chen, et al. Materials, Processing and reliability of low temperature bonding in 3D chip stacking. *Journal of Alloys and Compounds*, 2018, 750: 980–995.
[2] C T Ko, K Chen. Low temperature bonding technology for 3D integration. *Microelectronics Reliability*, 2012, 52: 302–311.
[3] K Tu, H Hsiao, C Chen. Transition from flip chip solder joint to 3D IC microbump: Its effect on microstructure anisotropy. *Microelectronics Reliability*, 2013, 53: 2–6.
[4] B Talebanpour, Z Huang, Z Chen, et al. Effect of joint scale and processing on the fracture of Sn–3Ag–0.5Cu solder joints: Application to micro–bumps in 3D packages. *Journal of Electronics Materials*, 2016, 45(1): 57–68.
[5] K Chu, Y Sohn, C Moon. A comparative study of Cu/Sn/Cu and Ni/Sn/Ni solder joints for low temperature stable transient liquid phase bonding. *Scripta Materialia*, 2015, 109: 113–117.
[6] W Chen, R Song, J Duh. Grain structure modification of Cu-Sn IMCs by applying Cu-Zn UBM on transient liquid-phase bonding in novel 3D-IC technologies. *Intermetallics*, 2017, 85: 170–175.
[7] L Zhang, Z Liu. Inhibition of intermetallic compounds growth at Sn–58Bi/Cu interface bearing CuZnAl memory particles (2–6 μm). *Journal of Materials Science: Materials in Electronics*, 2020, 31: 2466–2480.
[8] L Zhang, S Zhong. Effect of Ni_3Sn_4 on the thermo-mechanical fatigue life of solder joints in 3D IC. *Frontiers in Materials*, 2021, 8: 645782.
[9] Y Tian, N Wang, D Yang, et al. Stress analysis and structure optimization of IMC joints in 3D package. *Transactions of the China Welding Institution*, 2012, 33(8): 17–20. (in Chinese)
[10] C Lee, Y Lin, H Liu, et al. Reliability evaluation of ultra thin 3D-IC package under the coupling load effects of the manufacturing process and

temperature cycling test. *Microelectronic Engineering*, 2021, 244–246: 111572.
[11] X Long, Y Liu, Y Yao, et al. Constitutive behavior and life evaluation of solder joint under the multi-field loadings. AIP Advances, 2018, 8: 085001.
[12] S Annuar, R Mahmoodian, M Hamdi, et al. Intermetallic compounds in 3D integrated circuits technology: A brief review. *Science and Technology of Advanced Materials*, 2017, 18(1): 693–703.
[13] K Otiaba, R S Bhatti, N N Ekere, et al. Finite element analysis of the effect of silver content for Sn–Ag–Cu alloy compositions on thermal cycling reliability of solder die attach. *Engineering Failure Analysis*, 2013, 28: 192–207.
[14] P Lall, M Islam, N Singh, et al. Model for BGA and CSP reliability in automotive underhood applications. *IEEE Transactions on Components and Packaging Technologies*, 2004, 27(3): 585–593.
[15] L Zhang, L Sun, L Han, et al. Reliability of lead–free solder joints in WLCSP device with finite element simulation and Taguchi method. *International Journal of Nonlinear Sciences and Numerical Simulation*, 2014, 15(6): 405–410.
[16] L Zhang, J Han, C He, et al. Reliability behavior of lead–free soldered joints in electronic components. *Journal of Materials Science: Materials in Electronics*, 2013, 24(1): 172–190.
[17] M Samavatian, V Samavation, M Moayeri, et al. Effect of stress triaxiality on damage evolution of porous solder joints in IGBT discretes. *Journal of Manufacturing Processes*, 2018, 32: 57–64.
[18] X Li, Z Wang. Thermo-fatigue life evaluation of SnAgCu solder joints in flip chip assemblies. *Journal of Materials Processing Technology*, 2007, 183(1): 6–12.
[19] M Zarmai, N Ekere, C Oduoza, et al. Evaluation of thermo–mechanical damage and fatigue life of solar cell solder interconnections. *Robotics and Computer–Integrated Manufacturing*, 2017, 47: 37–43.
[20] L Zhang, S Xue, L Gao, et al. Creep behavior of SnAgCu solders with rare earth Ce doping. *Transactions of Nonferrous Metals Society of China*, 2010, 20(3): 412–417.
[21] L Zhang, J Han, Y Guo, et al. Effect of rare earth Ce on the fatigue life of SnAgCu solder joints in WLCSP device using FEM and experiments. *Materials Science and Engineering A*, 2014, 597: 219–224.
[22] M Xiong, L Zhang, P He, et al. Stress analysis and structural optimization of 3D IC package based on the Taguchi method. *Soldering & Surface Mount Technology*, 2019, 32(1): 42–47.
[23] Y Gu, T Nakamura. Interfacial delamination and fatigue life estimation of 3D solder bumps in flip–chip packages. *Microelectronics Reliability*, 2004, 44(3): 471–483.
[24] K Wu, S Lin, H Hung, et al. Reliability assessment of packaging solder joints under different thermal cycle loading rates. *IEEE Transactions on Device and Materials Reliability*, 2015, 15(3): 437–442.
[25] J Lau, S Lee. Modeling and analysis of 96.5Sn-3.5Ag-lead-free solder joints of wafer level chip scale package on buildup microvia printed circuit board. *IEEE Transactions on Electronics Packaging Manufacturing*, 2002, 25(1): 51–58.
[26] M Li, S Hong. Optimal parameter design for chip-on-film technology using the Taguchi method. *The International Journal of Advanced Manufacturing Technology*, 2005, 25(1–2): 145–153.
[27] T Tsai, M Liukkonen. Robust parameter design for the micro-BGA stencil printing process using a fuzzy logic-based Taguchi method. *Applied Soft Computing*, 2016, 48: 124–136.
[28] A Mertol. Application of the Taguchi method on the robust design of molded 225 plastic ball grid array packages. *IEEE Transactions on Components, Packaging, and Manufacturing Technology*, 1995, 18(4): 734–743.
[29] W Jong, S Chen, H Tsai, et al. The geometrical effects of bumps on the fatigue life of flip–chip packages by Taguchi method. *Journal of Reinforced Plastics and Composites*, 2006, 25(1): 99–114.
[30] A Syed. Accumulated creep strain and energy density based thermal fatigue life prediction models for SnAgCu solder joints. *54th Electronic Components and Technology Conference, Las Vegas, NV, USA,* 2004.
[31] L Zhang, J Han, Y Guo, et al. Fatigue life prediction of Sn-3.9Ag-0.6Cu soldered joints in WLCSP device. *Transactions of the China Welding Institution*, 2012, 33(3): 97–100. (**in Chinese**).
[32] N Jiang, L Zhang, W Long, et al. Influence of doping Ti particles on intermetallic compounds growth at Sn58Bi/Cu interface during solid–liquid diffusion. *Journal of Materials Science: Materials in Electronics*, 2021, 32(3): 341–3351.
[33] M Xiong, L Zhang, L Sun, et al. Effect of CuZnAl particles addition on microstructure of Cu/Sn58Bi/Cu TLP bonding solder joints. *Vacuum*, 2019, 167: 301–306.

Submit your manuscript to a SpringerOpen journal and benefit from:

► Convenient online submission
► Rigorous peer review
► Open access: articles freely available online
► High visibility within the field
► Retaining the copyright to your article

Submit your next manuscript at ► springeropen.com